Magnetic Force Microscopy Imaging of Current Paths

R. Yongsunthon[1], A. Stanishevsky[2], P. J. Rous[3], and E. D. Williams[1]
[1]Department of Physics, University of Maryland, College Park, MD 20742
[2]MRSEC, University of Maryland, College Park, MD 20742
[3]Department of Physics, University of Maryland, Baltimore Country, MD 20742

ABSTRACT

We demonstrate Magnetic Force Microscopy (MFM) imaging, at room temperature in air, of a 0.25mA DC current path in a 140nm-wide gold nanowire. The nanowire was created by focused ion beam milling of a 12μm wide Cr/Au line of 20nm/110nm Cr/Au thickness. Iterative fitting of the MFM data to an idealized model of the structure yielded a nanowire resistivity a factor of 3.5 higher than that of a control Cr/Au region which was unaffected by the ion beam processing. MFM imaging of an ion-implant patterned line shows current deflection around the implant region.

INTRODUCTION

We have previously demonstrated the ability of Magnetic Force Microscopy (MFM) to perform relative quantification [1,2] and observe current behaviors in conducting lines [3]. Additionally, a fully rigorous analysis involving both image deconvolution and inversion has been achieved and will be presented in future work [4,5]. Although our analysis has previously been limited to micron-scale current line widths, extension of these techniques to nanoscale devices and structures with spatial variations in resistivity is highly desirable. The key issues in making this extension are the conflicting demands of the sensitivity and spatial resolution needed to resolve nanoscale current paths.

Nanoscale resolution of MFM has been demonstrated for magnetic films [6-9]. However, the fields around nanoscale conducting lines containing nondestructive DC current densities are weak (typically <<mT) and thus require a relatively large magnetic tip volume to achieve sufficient signal to noise. Furthermore, the MFM response for standard vertical tip magnetization consists of sharp peaks of opposite polarity at the edges of the line, which result in mutual attenuation when the line width is less than the instrumental broadening due to the tip size. For example, with typical commercial MFM tips, such as the Digital Instruments MESP-HM tip, the magnetic film coats the entire tip pyramid (of about 8μm height and 8μm base) resulting in a large magnetic volume but limited spatial resolution. Given the long-range nature of the weak magnetic interaction between the MFM tip and current-carrying line, it will clearly push the limits of the present instrumental capability to resolve current paths at the nanoscale. We will here demonstrate measurements at the scale of 100 nm width wires, using a commercial MFM operated in air. The limits determined here may be improved with higher resolution tips, with more selectively placed magnetic coatings [6-9], although gains in spatial resolution are likely to be offset by smaller signal sensitivity. The loss of sensitivity could be compensated, at least in part, by performing the measurement in vacuum and/or at low temperature to increase the sensitivity to the magnetic interaction [10]. However, such instruments have not yet been demonstrated for current-carrying devices, which are subject to the difficulties discussed above, as well as generating heat due to power dissipation.

EXPERIMENTAL DETAILS

Experiments were performed using a Digital Instruments Multimode, operated in tapping (intermittent non-contact) mode with standard MFM phase detection. The signal detected is proportional to the curvature of the magnetic field component perpendicular to the sample plane, integrated over the magnetic tip volume. The magnetic tips used are commercially available Co/Cr coated Digital Instruments MESP-HM tips, magnetized along the tip axis, perpendicular to the sample surface. All magnetic phase data is interpreted relative to a known reference standard, thereby avoiding the need for exact knowledge of the tip magnetization.

The nanowire sample, shown in Fig. 1, was fabricated using a combination of standard photolithography, liftoff, and focused-ion beam (FIB) milling techniques. The Cr/Au metal line, chosen for chemical and physical stability, was 12μm wide, as defined by lift-off. The thickness of the Cr was 20nm, and the Au was 110nm. Additional structures, such as the (2x6) μm^2 rectangular defects were fabricated by FIB milling [11]. The lower rectangular defect was milled to leave a 140nm conducting line width on the left edge of the line. Ion milling was performed with 50 kV Ga^+ ions using a Micrion 2500 FIB machine with a 5 nm beam column. A serpentine beam scanning procedure and relatively low (~30 pA) ion current were chosen to provide a better defect shape.

MFM measurements were made with typical currents in the individual lines of 30mA, corresponding to current densities on the order of $2\text{-}5\times10^6 A/cm^2$. To exclude topographical artifacts, the MFM phase measurements were performed in Digital Instruments Interleave Linear Lift Mode, using a lift height of 200nm (which corresponds to a separation of 110nm between the tip and the top surface of the Cr/Au line). To exclude phase response due to electrostatic forces, the potential between the tip and sample was nulled by an external voltage divider, as discussed in previous work [1,2].

DISCUSSION

The nanowire can be seen in the lower left of the topographic image of Figure 1a. The effect of the nanowire is not immediately apparent in the MFM image to the left of Fig. 1b, which shows the expected MFM contrast at the line edges where the magnetic field must curve into or out of the sample plane. There is significantly higher contrast at the inner edge of the rectangular defects than at the line edge on the side opposite the defect, due to a nonuniform, localized increase in current density, discussed in previous work [3]. Figure 1b presents a close-up of the 140nm line. Halfway through the image scan, the current in the line was reversed and the expected reversal in MFM signal polarity was observed. A separate image of the topography, taken with a non-magnetic, topography-specific OTESP tip, has yielded a nanowire width of 140nm and a remainder (region not milled away) line width of 6μm. Given the known total current of 40mA flowing through the structure and the relative line widths of the nanowire and the wire, we may estimate that 2.3% of the total current, or 0.9mA is flowing through the line. This value is likely to be an upper estimate, since the nanowire suffered damage during the ion milling and is probably more resistive than the rest of the line. At a current of 1mA and a tip-sample separation of about 100nm, this nanowire would produce a field of 0.5mT, a field gradient of 4900 T/m, and a field curvature of 7×10^{10} T/m^2. Although the nanowire line width is 140nm, the peak centers of the MFM signal shown are separated by approximately 180nm,

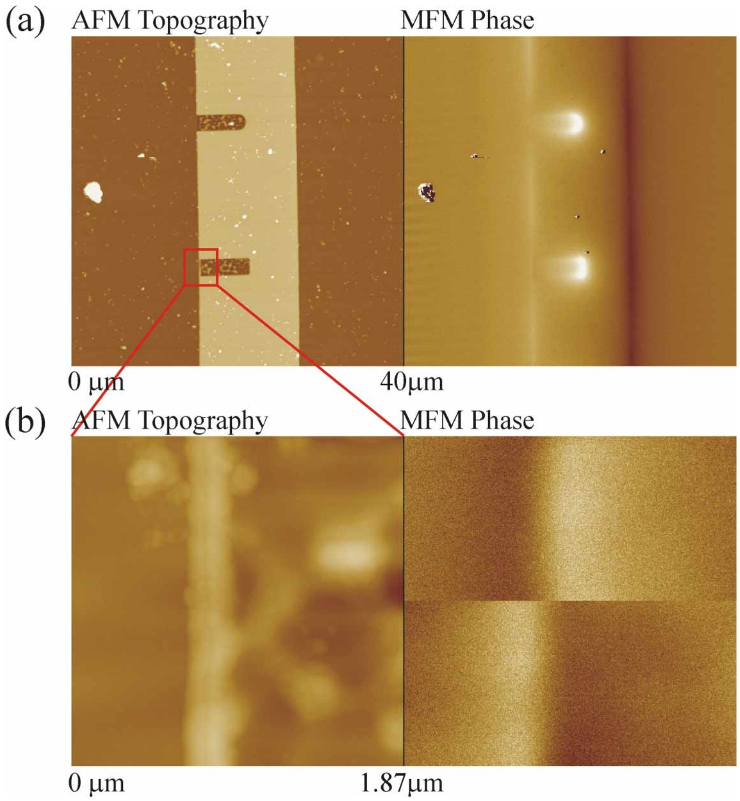

Figure 1: 140nm nanowire created by focused ion beam milling

a) The 12µm wide, 130nm thick Cr/Au line contains (2x6) μm^2 notches where the corners have varying radii of curvature. In the bottom notch, the milling left a 140nm conducting line width. The total current in the 12µm line is 40 mA.
b) The polarity in the MFM signal of the close-up of the nanowire changes as the current is reversed, confirming that the signal is due to current flowing through the nanowire. The apparent physical line width is larger than the actual 140nm width due to tip convolution effects.

demonstrating limits in magnetic spatial resolution resulting from the large tip size and tip-sample separation.

The relative MFM signal strength at the 140 nm line and in the defect-free part of the 12µm line can be used to determine the relative current levels in the two lines. This in turn may be used to deduce the relative resistivity change due to processing techniques such as the focused ion beam milling performed on this sample. Given a simple sample configuration and barring the need to extract a full two-dimensional map of the current distribution, the unprocessed MFM data may be interpreted by iterative fitting to a simple model.

The model consists of a 140nm wide line parallel to a 6µm wide line and separated by 6µm, assumed to be infinitely long with uniform current density and thus analytically calculable. The nanowire is sufficiently far from the 6µm line that it is negligibly affected by the inhomogeneous current density in the larger line. To deduce the current running in the wire, the calculation was convolved with an estimated two-dimensional instrumental response function.

Using an average of 15 line scans, corresponding to a 1.2 μm line segment length, yields the signal shown as the thick gray line in Fig. 2a. The nanowire signal appears as a small feature near 15μm and the signal from the 6μm wide remainder segment of the line is located between 20 μm and 30 μm. A portion of the line sufficiently far from the nanowire region is used as a reference for signal normalization. The experimental ratio of MFM peak heights is MFM_{nano}=0.062$MFM_{ref.}$ To evaluate the amount of current flowing through the nanowire, the current density in the nanowire is adjusted until the shape and relative amplitude of the forward convolution is as consistent as possible with the actual data. Using a resistivity 3 times that of the remaining line (e.g. assuming a current density three times smaller than the value of 0.9 mA deduced from geometrical consideration), we obtain the forward convolution of Fig. 2a, where the data is the thick gray line and the forward convolution is the thin black line; the theoretical ratio for this scenario is MFM_{nano}=0.072MFM_{ref}. Using a resistivity of 4 yields curves of similar shape and magnitude, with a ratio of MFM_{nano}=0.053MFM_{ref}. A simple interpolation then suggests that the resistivity is ~3.5 times higher than the undamaged line, which suggests a nanowire current of MFM_{nano}=0.072MFM_{ref}. A zoom-in near the nanowire is shown in Fig. 2b, with the data plotted in bold gray and the resistivity 3 and resistivity 4 calculations in solid black and dotted black, respectively.

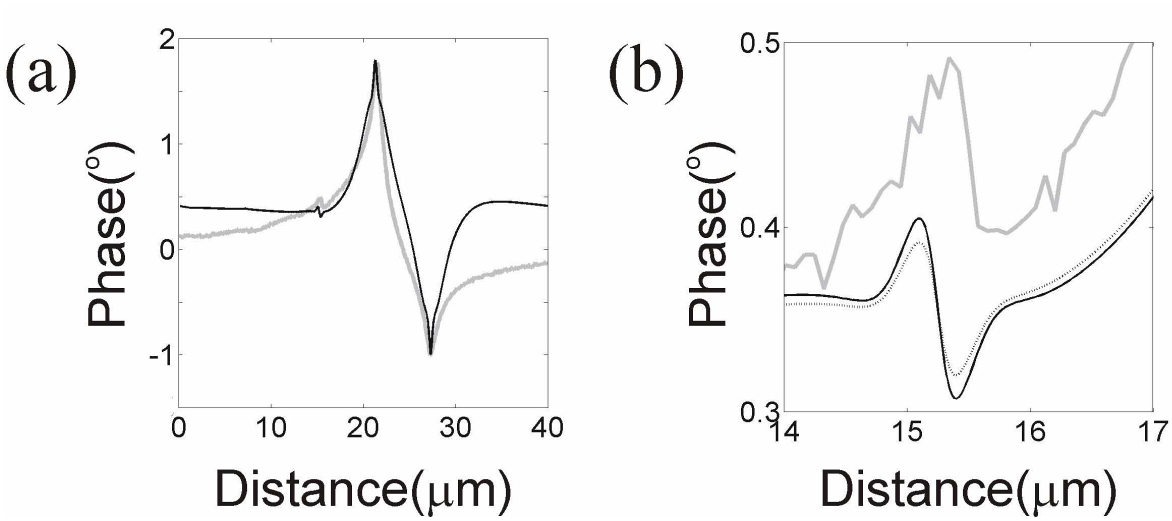

Figure 2: Iterative fitting to the MFM signal profile from the 140nm wire and the 6μm remainder wire

Experimental data is plotted in gray and model calculations are plotted in black. The signal from the 6 μm segment peaks at 22 and 28 μm, and the signal from the nanowire is between 15 and 16 μm.

a) Comparison of experimental data with the a calculated curvature obtained using a nanowire resistivity 4 times that of the remaining line, and a convolution with an estimated 2-D instrumental response function. The units of the calculation were normalized to the units and amplitude of the experimental data (degrees).
b) Close-up, where the data is plotted in bold gray and the model calculations for a factor of 3 and a factor of 4 increase in resistivity are shown with dotted black and solid black lines, respectively.

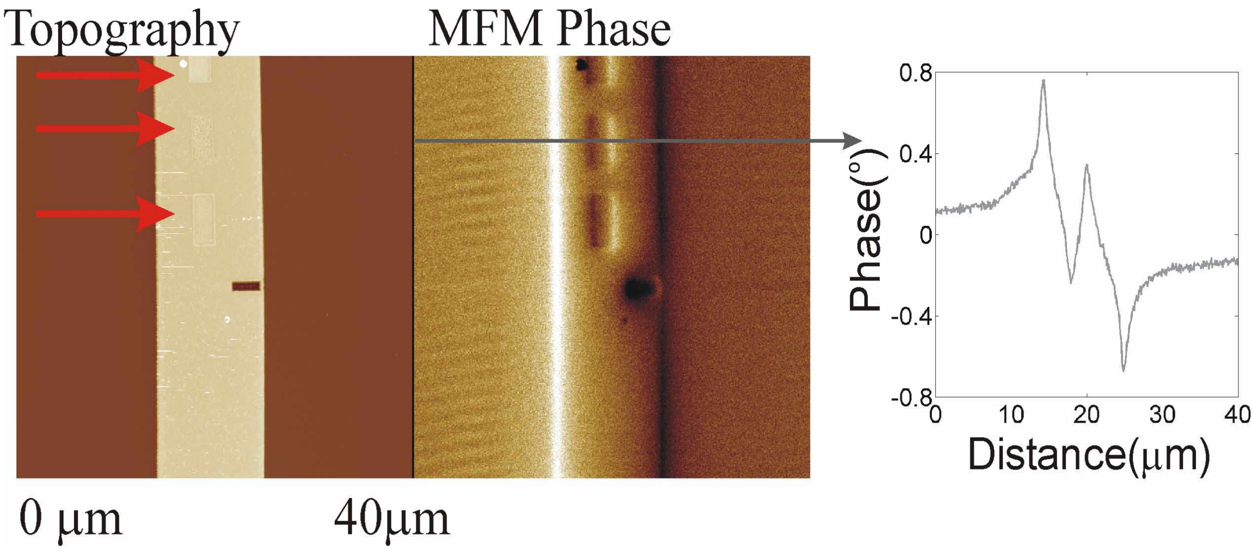

Figure 3: Topography and MFM phase images of areas intentionally damaged by focused-ion beam dosing: 12µm wide line composed of 80nm/20nm Ti/Au with a fiducial rectangular vacancy created by ion milling. In the leftmost image, the three red arrows indicate the location of three (2x6)μm^2 regions implanted with varying ion beam doses to induce material damage with minimal material removal. The MFM peaks around the boundaries of the implanted regions indicate deflections in current flow which result from increased resistivity of the ion beam damaged regions. The line scan on the right is the average of 20 MFM line scans taken from the center of the middle implantation region, as indicated by the gray arrow.

It seems reasonable to conclude that the increase in resistivity is caused by ion implantation damage during the ion milling process. To confirm this possibility, a Ti/Au wire was fabricated and patterned with an implant under conditions which minimized ion milling. The result is shown in Fig. 3. In the upper half of the sample, three (2x6)μm^2 regions were implanted with varying ion beam doses to induce material damage with minimal material removal (highlighted in the leftmost image by the arrows). The implant structures are nearly invisible in topography, displaying a height change of less than 10nm. However, the location of the implants is clearly visible in the MFM phase image, in which intensity highlights the boundaries of the implanted regions. The intensity highlights indicate deflection of current into the regions on either side of the implant regions, consistent with increased resistivity of the ion beam damaged regions. An average of 20 MFM line scans, corresponding to a 1.6µm length, taken from the center of the middle implanted region is shown on the right of Fig. 3. Although there may be a small attenuation effect due to tip convolution, the lower contrast of the MFM peaks at the implantation boundaries, relative to the MFM peaks at the line edges, is primarily a result of the lowered (but nonzero) current density in the higher resistance implantation regions. The ratio of the implantation MFM peaks to that of the reference peaks, from a region far from the implantation, is $MFM_{implant}=0.41MFM_{ref}$. Using scaling analysis similar to that of the nanowire above, the resistivity of the middle implantation region is estimated as a factor of 2.4 higher than that of the Ti/Au region unaffected by the ion dosing.

CONCLUSION

Using commercial instrumentation, we have demonstrated the ability of commercial Magnetic Force Microscopy to detect the 0.25mA DC current path in a 140nm-wide gold nanowire and determine relative resistivity change of the conducting material, as induced by focused ion beam dosing. These measurements suggest that deconvolution and inversion techniques we have developed for determining the spatial distribution of current in micron-scale current-carrying lines can be extended to nanoscale regimes and applied to nanoscale devices.

We have also directly demonstrated the deflection of electrical current around metal regions damaged by ion implantation. These results show that, in addition to resolving current paths in nanoscale conductors, MFM can be used to detect nanoscale changes in material properties, e.g. due to resistivity perturbations induced by innovative processing techniques or contact resistance issues in nanoscale devices.

ACKNOWLEDGEMENTS

This work has been supported by the US Department of Energy grant DE-FG02-01ER45939 and by the NSF-Materials Research Science and Engineering Center under grant DMR-00-80008.

REFERENCES

1. R. Yongsunthon, J. McCoy, and E. D. Williams, J. Vac. Sci. Technol. 19, 1763-1768 (2001).
2. R. Yongsunthon, J. McCoy, and E. D. Williams, ULSI Metrology Conference Proceedings 550, 630-634 (2001).
3. R. Yongsunthon, A. Stanishevsky, J. McCoy, and E. D. Williams, Appl. Phys. Lett. 78, 2661-2663 (2001).
4. R. Yongsunthon, P. J. Rous, A. Stanishevsky, and E. D. Williams, unpublished.
5. P. J. Rous, R. Yongsunthon, A. Stanishevsky, and E. D. Williams, unpublished.
6. G. D. Skidmore and E. D. Dahlberg, Appl. Phys. Lett. 71, 3293-3295 (1997).
7. P. J. A. v. Schendel, H. J. Hug, B. Stiefel, S. Martin, and H.-J. Guntherodt, J. Appl. Phys. 99, 435-445 (2000).
8. T. Larsen, K. Moloni, F. Flack, M. A. Eriksson, M. G. Lagally, and C. T. Black, Appl. Phys. Lett. 80, 1996-1998 (2002).
9. P. Eames, E. D. Dahlberg, and K. Moloni, unpublished.
10. M. Liebmann, A. Schwarz, S. M. Langkat, and R. Wiesendanger, Review of Scientific Instruments 73, 3508-3514 (2002).
11. J. Melngailis, J. Vac. Sci.Technol. B 5, 469-495 (1987).